Synthesis and Characterization of Thiolato-Bridged Trinuclear Heterometal Complexes with 2-[(3-Aminopropyl)amino]ethanethiol

Masahiro Mikuriya,* Hideyuki Tsutsumi, Ryoji Nukada, Makoto Handa,† and Yasuyoshi Sayama

Department of Chemistry, School of Science, Kwansei Gakuin University, Uegahara, Nishinomiya 662

†Department of Material Science, Interdisciplinary Faculty of Science and Engineering, Shimane University, Nishikawatsu, Matsue 690

(Received July 16, 1996)

A series of ten trinuclear heterometal complexes with 2-[(3-aminopropyl)amino]ethanethiol (HL), $[(M_AL_2)_2M_B](ClO_4)_2\cdot 2dmac\cdot 2X$ ($[M_A, M_B] = [Mn, Zn]$, [Mn, Cd], [Fe, Zn], [Fe, Cd], [Fe, Hg], [Co, Zn] [Co, Cd], [Ni, Zn], [Ni, Cd], [Ni, Hg]; dmac = *N*,*N*-dimethylacetamide, $X = H_2O$ or CH_3OH), have been synthesized and characterized by infrared and electronic spectroscopies, temperature dependence of magnetic susceptibilities (80—300 K), and single-crystal X-ray diffraction technique. Each complex has a thiolato-bridged heterotrinuclear structure which shows a linear arrangement of *Oh*(M_A)–*Td*(M_B)–*Oh*(M_A). The spectral and magnetic properties were discussed in relation to the crystal structures.

There has been considerable research interest in the coordination chemistry of thiolato-bridged metal complexes with chelating thiolate ligands over the past three decades. In 1962 Bush et al. prepared linear-type thiolato-bridged trinuclear complexes using didentate thiolate ligand, 2-aminoethanethiol (Haet).[1—3] These complexes are formed by the chelating thiolate ligand which forms mononuclear complexes of the type $M(aet)_3$. These mononuclear species acting as ligands toward other metal ions afford linear-type homo or heterotrinuclear complexes, $[\{M(aet)_3\}_2M']$ showing a linear arrangement of *Oh*(M)–*Oh*(M′)–*Oh*(M).[4] Trinuclear metal complexes are also known in several different formula types, including $M_3(aet)_4$ and $M_3(aet)_6$ for several metal ions.[5—11] These complexes have been the subject of a number of studies. Recently, Konno, Okamoto, and Hidaka have prepared a number of interesting polynuclear metal complexes by using this binding ability of the coordinated thiolato sulfur atoms.[12—26] On the other hand, metal complexes with a related tridentate thiolate ligand, 2-[(3-aminopropyl)amino]ethanethiol (HL) have not been explored.[27,28] Therefore we have continued studying thiolato-bridged metal complexes by using this thiolate ligand.[29—37] In the course of this study, we have found that the HL ligand forms a novel linear-type trinuclear complex, $[(ML_2)_2M]^{2+}$, for Mn^{2+}, Fe^{2+}, and Co^{2+} ions.[35,36,38] In these complexes, the three metal ions are arranged in a linear array like the trinuclear complexes with 2-aminoethanethiol, but the coordination environment is different from the case with the $[\{M(aet)_3\}_2M']$ complexes. The central metal atom is situated in a tetrahedral geometry, coordinated by four sulfur atoms from the two terminal *mer*-$[ML_2]$ subunits where the two terminal metal atoms take octahedral N_4S_2 environments forming a linear *Oh*(M)–*Td*(M)–*Oh*(M) arrangement. By using these different coordination environments we have expected to be able to direct different metal ions, with specificity, to different binding sites within the trinuclear molecule to form a new trinuclear heterometal complex, $[(M_AL_2)_2M_B]^{2+}$. In this work, we have started from a controlled mixture of metal salts of Mn^{2+}, Fe^{2+}, Co^{2+}, or Ni^{2+} ion which prefers to take an octahedral geometry and some other appropriate metal salt of Zn^{2+}, Cd^{2+}, or Hg^{2+} ion which prefers to take a tetrahedral geometry. Two metal ions, $M_A = Mn^{2+}$, Fe^{2+}, Co^{2+}, or Ni^{2+}, are directed to the outer positions of the complexes and the central site is reserved for the other metal ion $M_B = Zn^{2+}$, Cd^{2+}, or Hg^{2+}. We report here facile synthesis of new thiolato-bridged trinuclear heterometal complexes by using one-pot reaction.

Experimental

Synthesis of the Complexes. Unless otherwise specified, commercial chemicals were used as supplied. Iron(II) chloride tetrahydrate was obtained from Aldrich Chemical Co. and mercury(II) chloride was purchased from Ishizu Seiyaku Co. All other materials were obtained from Kishida Chemical Co. Methanol was dried using standard laboratory techniques. 2-[(3-Aminopropyl)amino]-ethanethiol and iron(II) tetrafluoroborate hexahydrate were prepared according to published procedures.[27,39] All operations were done under an atmosphere of argon using standard Schlenk techniques.

$[(MnL_2)_2Zn](ClO_4)_2\cdot 2dmac\cdot 2CH_3OH$ (1). To a methanol (4 cm^3)-*N*,*N*-dimethylacetamide (1 cm^3) solution of HL (81 mg, 0.60 mmol) two drops of triethylamine were added. A solution of managanese(II) perchlorate hexahydrate (146 mg, 0.40 mmol) and zinc(II) perchlorate hexahydrate (75 mg, 0.20 mmol) in a mixture of methanol (4 cm^3) and *N*,*N*-dimethylacetamide (1 cm^3) was added dropwise with stirring. The resulting clear solution was left to

stand at −20 °C for several days. Colorless plates were deposited; they were collected by filtration (yield 84 mg, 52% based on HL). Found: C, 31.14; H, 7.01; N, 11.93; Mn, 9.6; Zn, 6.1%. Calcd for $C_{30}H_{78}Cl_2Mn_2N_{10}O_{12}S_4Zn$: C, 31.46; H, 6.86; N, 12.23; Mn, 9.6; Zn, 5.7%. IR (KBr) ν/cm^{-1} ν(NH) 3222(m), 3170(m), ν(CH) 2918(m), 2846(m), $\nu(ClO_4)$ 1143(s), 1112(s), 1089(s), 628(s). λ_M(DMF (*N*,*N*-dimethylformamide))/S mol^{-1} cm^2 136 (lit, range for 2 : 1 electrolytes,[40] 130—170 S mol^{-1} cm^2). Electronic spectrum in DMF: no peak was found in the range 300—1650 nm. Diffuse reflectance spectrum: λ_{max}/nm 1197, 1564.

[(MnL$_2$)$_2$Cd](ClO$_4$)$_2$·2dmac·2H$_2$O (2). This complex was prepared in the same way as that for [(MnL$_2$)$_2$Zn](ClO$_4$)$_2$·2dmac·2CH$_3$OH except for using cadmium(II) perchlorate hexahydrate instead of zinc(II) perchlorate hexahydrate (yield 116 mg, 59% based on HL). Found: C, 28.45; H, 6.06; N, 11.56; Mn, 8.9; Cd, 10.4%. Calcd for $C_{28}H_{74}Cl_2Mn_2N_{10}O_{12}S_4Cd$: C, 28.88; H, 6.41; N, 12.03; Mn, 9.4; Cd, 9.7%. IR (KBr) ν/cm^{-1} ν(NH) 3222(m), 3166(m), ν(CH) 2916(m), 2880(m), 2846(m), $\nu(ClO_4)$ 1141(s), 1110(s), 1089(s), 627(s). λ_M(*N*,*N*-dimethylformamide)/S mol^{-1} cm^2 132. Electronic spectrum in DMF: No peak was found in the range 300—1650 nm. Diffuse reflectance spectrum: λ_{max}/nm 1194, 1556.

[(FeL$_2$)$_2$Zn](ClO$_4$)$_2$·2dmac·2CH$_3$OH (3). HL (87 mg, 0.65 mmol) and 2 drops of triethylamine were dissolved in a mixture of methanol (4 cm^3) and *N*,*N*-dimethylacetamide (1 cm^3). A solution of ion(II) chloride tetrahydrate (86 mg, 0.43 mmol), zinc(II) perchlorate hexahydrate (80 mg, 0.21 mmol), and sodium perchlorate (106 mg, 0.87 mmol) in methanol (4 cm^3)–*N*,*N*-dimethylacetamide (1 cm^3) was added dropwise with stirring. The resulting orange solution was left to stand at −20 °C for several days. Orange plates were deposited; they were collected by filtration (yield 83 mg, 45% based on HL). Found: C, 29.08; H, 6.53; N, 12.06; Fe, 10.7; Zn, 5.9%. Calcd for $C_{25}H_{65}Cl_2Fe_2N_9O_{10}S_4Zn$: C, 29.21; H, 6.37; N, 12.26; Fe, 10.9; Zn, 6.4%. IR(KBr) ν/cm^{-1} ν(NH) 3203(m), 3180(m), 3130(m), ν(CH) 2920(m), 2872(m), 2844(m), $\nu(ClO_4)$ 1142(s), 1113(s), 1082(s), 627(s). Diffuse reflectance spectrum: λ_{max}/nm 870, 1029, 1563.

[(FeL$_2$)$_2$Cd](ClO$_4$)$_2$·2dmac·2H$_2$O (4). This complex was prepared in the same way as that for [(FeL$_2$)$_2$Zn](ClO$_4$)$_2$·2dmac·2CH$_3$OH except for using cadmium(II) perchlorate hexahydrate instead of zinc(II) perchlorate hexahydrate (yield 72 mg, 38% based on HL). Found: C, 29.33; H, 6.62; N, 11.86; Fe, 10.5; Cd, 10.6%. Calcd for $C_{28}H_{70}CdCl_2Fe_2N_{10}O_{10}S_4$: C, 29.76; H, 6.60; N, 12.36; Fe, 9.9; Cd, 10.0%. IR (KBr) ν/cm^{-1} ν(NH) 3212(m), 3178(m), 3135(m), ν(CH) 2916(m), 2870(m), 2844(m), $\nu(ClO_4)$ 1142(s), 1111(s), 1086(s), 627(s). Diffuse reflectance spectrum: λ_{max}/nm 880, 1060, 1560.

[(FeL$_2$)$_2$Hg](ClO$_4$)$_2$·2dmac·2H$_2$O (5). To a methanol (4 cm^3)-*N*,*N*-dimethylacetamide (1 cm^3) solution of HL (102 mg, 0.76 mmol) one drop of triethylamine was added. A solution of iron(II) tetrafluoroborate hexahydrate (171 mg, 0.51 mmol), mercury(II) chloride (69 mg, 0.26 mmol), and sodium perchlorate (186 mg, 1.52 mmol) in a mixture of methanol (4 cm^3) and *N*,*N*-dimethylacetamide (1 cm^3) was added dropwise with stirring. The resulting yellow solution was left to stand at room temperature for several days. Yellow crystals and a gelatinous white precipitate were deposited; the yellow crystals were collected by decantation. Recrystallization from methanol (4 cm^3)–*N*,*N*-dimethylacetamide (1.5 cm^3) yielded 68 mg (29% based on HL) of **5** as yellow plates. Found: C, 26.35; H, 5.93; N, 10.66; Fe, 8.8%. Calcd for $C_{28}H_{74}Cl_2Fe_2HgN_{10}O_{12}S_4$: C, 26.81; H, 5.95; N, 11.17; Fe, 8.9%. IR (KBr) ν/cm^{-1} ν(NH) 3212(m), 3175(m), 3139(m), ν(CH) 2918(m), 2872(m), 2842(m), $\nu(ClO_4)$ 1143(s), 1111(s), 1087(s), 627(s). Diffuse reflectance spectrum: λ_{max}/nm 918, 1066, 1564.

[(CoL$_2$)$_2$Zn](ClO$_4$)$_2$·2dmac·2CH$_3$OH (6). HL (119 mg, 0.89 mmol) and 12 drops of triethylamine were dissolved in a mixture of methanol (4 cm^3) and *N*,*N*-dimethylacetamide (1 cm^3). A solution of cobalt(II) perchlorate hexahydrate (81 mg, 0.22 mmol) and zinc(II) perchlorate hexahydrate (54 mg, 0.15 mmol) in methanol (4 cm^3)–*N*,*N*-dimethylacetamide (1 cm^3) was added dropwise with stirring. The resulting purple solution was left to stand at −20 °C for several days. Purple plates were deposited; they were collected by filtration (yield 84 mg, 66% based on Co(ClO$_4$)$_4$·6H$_2$O). Found: C, 29.38; H, 6.65; N, 11.84; Co, 11.0; Zn, 6.1%. Calcd for $C_{25}H_{65}Cl_2Co_2N_9O_{10}S_4Zn$: C, 29.03; H, 6.33; N, 12.19; Co, 10.8; Zn, 6.0%. IR (KBr) ν/cm^{-1} ν(NH) 3184(m), 3140(m), ν(CH) 2918(m), 2865(m), 2846(m), $\nu(ClO_4)$ 1143(s), 1111(s), 1086(s), 626(s). λ_M(*N*,*N*-dimethylformamide)/S mol^{-1} cm^2 137. Electronic spectrum in DMF: λ_{max}/nm (ε/dm^3 mol^{-1} cm^{-1}) 513 (79), 786 (3.6), 1078 (16), 1421 (5.6), 1556 (4.1). Diffuse reflectance spectrum: λ_{max}/nm 512, 783, 1081, 1563.

[(CoL$_2$)$_2$Cd](ClO$_4$)$_2$·2dmac·2H$_2$O (7). HL (90 mg, 0.67 mmol) and 2 drops of triethylamine were dissolved in a mixture of methanol (4 cm^3) and *N*,*N*-dimethylacetamide (1 cm^3). A solution of cobalt(II) perchlorate hexahydrate (164 mg, 0.45 mmol) and cadmium(II) perchlorate hexahydrate (94 mg, 0.22 mmol) in methanol (4 cm^3)–*N*,*N*-dimethylacetamide (1 cm^3) was added dropwise with stirring. The resulting purple solution was left to stand at −20 °C for several days. Purple plates were deposited; they were collected by filtration (yield 83 mg, 45% based on HL). Found: C, 28.69; H, 6.35; N, 11.93; Co, 10.0; Cd, 10.0%. Calcd for $C_{28}H_{74}Cl_2CdCo_2N_{10}O_{12}S_4$: C, 28.69; H, 6.36; N, 11.95; Co, 10.1; Cd, 9.6%. IR (KBr) ν/cm^{-1} ν(NH) 3192(m), 3129(m), ν(CH) 2920(m), 2860(m), $\nu(ClO_4)$ 1141(s), 1109(s), 1089(s), 626(s). λ_M(*N*,*N*-dimethylformamide)/S mol^{-1} cm^2 137. Electronic spectrum in DMF: λ_{max}/nm (ε/dm^3 mol^{-1} cm^{-1}) 514 (78), 1105 (15). Diffuse reflectance spectrum: λ_{max}/nm 514, 1109, 1563.

[(NiL$_2$)$_2$Zn](ClO$_4$)$_2$·2dmac·2CH$_3$OH (8). HL (87 mg, 0.65 mmol) and 2 drops of triethylamine were dissolved in a mixture of methanol (4 cm^3) and *N*,*N*-dimethylacetamide (1 cm^3). A solution of nickel(II) perchlorate hexahydrate (79 mg, 0.22 mmol) and zinc(II) perchlorate hexahydrate (40 mg, 0.11 mmol) in methanol (4 cm^3)–*N*,*N*-dimethylacetamide (1 cm^3) was added dropwise with stirring. The resulting blue solution was left to stand at room temperature for several days. Blue plates were deposited; they were collected by filtration (yield 94 mg, 76% based on Ni(ClO$_4$)$_2$·6H$_2$O). Found: C, 29.55; H, 6.64; N, 11.85; Ni, 10.9; Zn, 6.6%. Calcd for $C_{25}H_{65}Cl_2Ni_2N_9O_{10}S_4Zn$: C, 29.05; H, 6.34; N, 12.19; Ni, 11.4; Zn, 6.3%. IR (KBr) ν/cm^{-1} ν(NH) 3220(m), 3184(m), 3144(m), ν(CH) 2920(m), 2848 (m), $\nu(ClO_4)$ 1145(s), 1110(s), 1085(s), 627(s). λ_M(*N*,*N*-dimethylformamide)/S mol^{-1} cm^2 135. Electronic spectrum in DMF: λ_{max}/nm (ε/dm^3 mol^{-1} cm^{-1}) 369 (149), 586 (31), 920 (26). Diffuse reflectance spectrum: λ_{max}/nm 369, 592, 931, 1563.

[(NiL$_2$)$_2$Cd](ClO$_4$)·2dmac·2H$_2$O (9). This complex was prepared in the same way as that for [(NiL$_2$)$_2$Zn](ClO$_4$)$_2$·2dmac·2CH$_3$OH except for using cadmium(II) perchlorate hexahydrate instead of zinc(II) perchlorate hexahydrate (yield 107 mg, 89% based on Ni(ClO$_4$)$_2$·6H$_2$O). Found: C, 29.30; H, 6.45; N, 11.92; Ni, 10.1; Cd, 9.5%. Calcd for $C_{28}H_{74}Cl_2Ni_2N_{10}O_{12}S_4Cd$: C, 28.70; H, 6.34; N, 11.95; Ni, 10.0; Cd, 9.6%. IR (KBr) ν/cm^{-1} ν(NH) 3220(m), 3175(m), ν(CH) 2918(m), 2850(m), $\nu(ClO_4)$ 1141(s), 1110(s), 1089(s), 627(s). λ_M(*N*,*N*-dimethylformamide)/S mol^{-1} cm^2 149. Electronic spectrum in DMF: λ_{max}/nm

(ε/dm^3 mol^{-1} cm^{-1}) 371 (64), 591 (24), 930 (28). Diffuse reflectance spectrum: λ_{max}/nm 369, 593, 933, 1563.

$[(NiL_2)_2Hg](ClO_4)_2\cdot 2dmac\cdot 2H_2O$ (10). To a methanol (4 cm^3)–*N*,*N*-dimethylacetamide (1 cm^3) solution of HL (101 mg, 0.75 mmol) two drops of triethylamine were added. A solution of nickel(II) perchlorate hexahydrate (183 mg, 0.50 mmol), mercury(II) chloride (68 mg, 0.25 mmol), and sodium perchlorate (61 mg, 0.50 mmol) in a mixture of methanol (4 cm^3) and *N*,*N*-dimethylacetamide (1 cm^3) was added dropwise with stirring. The resulting blue solution was left to stand at room temperature for several days. Blue crystals were deposited; they were collected by decantation. Recrystallization from methanol (4 cm^3)–*N*,*N*-dimethylacetamide (3 cm^3) yielded 120 mg (51% based on HL) of **10** as blue plates. Found: C, 26.70; H, 5.91; N, 11.05; Ni, 9.7%. Calcd for $C_{28}H_{74}Cl_2HgN_{10}Ni_2O_{12}S_4$: C, 26.69; H, 5.92; N, 11.12; Ni, 9.3%. IR (KBr) ν/cm^{-1} ν(NH) 3216(m), 3180(m), 3136(m), ν(CH) 2918(m), 2848(m), ν(ClO_4) 1141(s), 1112(s), 1086(s), 626(s). λ_M(*N*,*N*-dimethylformamide)/S mol^{-1} cm^2 146. Electronic spectrum in DMF: λ_{max}/nm (ε/dm^3 mol^{-1} cm^{-1}) 595 (26), 920 (28). Diffuse reflectance spectrum: λ_{max}/nm 380sh, 593, 939, 1565.

Measurements. Carbon, hydrogen, and nitrogen analyses were carried out using a Perkin–Elmer 2400 Series II CHNS/O Analyzer. Metal analysis was carried out with a Hitachi Atomic Absorption-Flame Spectrophotometer Model 508A. Infrared spectra were measured with a JASCO Infrared Spectrometer model IR700 in the 4000—400 cm^{-1} region on a KBr disk. Electronic conductivities were measured on a Horiba conductivity meter DS-14. Electronic spectra were measured with a Shimadzu UV-vis-NIR Recording Spectrophotometer Model UV-3100. The magnetic susceptibilities were measured over the 80—300 K temperature range. The susceptibilities were corrected for the diamagnetism of the constituent atoms using Pascal's constants.[41] The effective magnetic moments were calculated from the equation $\mu_{eff} = 2.828\sqrt{\chi_M T}$, where χ_M is the molar magnetic susceptibility.

X-Ray Crystal Structure Analysis. Unit-cell parameters and intensities were measured on an Enraf–Nonius CAD4 diffractometer using graphite-monochromated Mo $K\alpha$ radiation at 25±1 °C. Unit-cell parameters were determined by a least-squares refinement based on 25 reflections with $20 \leq 2\theta \leq 30^\circ$. Crystal data and details of the data collection are given in Table 1. Intensity data were corrected for Lorentz-polarization effects, but not for absorption. The structures were solved by the direct methods and refined by the full-matrix least-squares methods. All the non-hydrogen atoms were refined with anisotropic thermal parameters. The hydrogen atoms were inserted at their calculated positions and fixed at these positions. The final discrepancy factors, $R = \sum||F_o| - |F_c||/\sum|F_o|$, $R_w = [w(|F_o| - |F_c|)^2/\sum w|F_o|^2]^{1/2}$, are listed in Table 1. The weighting scheme, $w = 1/[\sigma^2(|F_o|) + (0.02|F_o|)^2 + 1.0]$, was employed. All of the calculations were carried out on a VAX station 4000 90A computer using a MolEN program package.[42] The atomic coordinates, thermal parameters, bond distances and angles, and $F_o - F_c$ tables were deposited as Document No. 69067 at the Office of the Editor of Bull. Chem. Soc. Jpn.

Results and Discussion

In recent reports, we described syntheses and characterizations of related homometal complexes with 2-[(3-aminopropyl)amino]ethanethiol, HL.[35,36,38] In these cases, we obtained trinuclear Mn(II),[35] Fe(II),[36] Co(II),[38] and Ni(II)[38] complexes which show a linear arrangement of the three metal atoms with a *Oh–Td–Oh* geometry. In this study, the reaction of 2-[(3-aminopropyl)amino]ethanethiol (HL) with an appropriate mixture of two kinds of metal ions afforded the desired trinuclear heterometal complexes $[(M_AL_2)_2M_B](ClO_4)_2\cdot 2dmac\cdot 2X$ (M_A = Mn, Fe, Co, Ni; M_B = Zn, Cd, Hg; dmac = *N*,*N*-dimethylacetamide, X = H_2O or CH_3OH). When the reaction was done under the HL : M_A : M_B = 4 : 2 : 1 molar ratio, the product was occasionally contaminated with small amount of homometal species. Therefore we accommodated the molar ratio in each case to avoid the contamination. Crystal suitable for X-ray crystallography were obtained from methanol–*N*,*N*-dimethylacetamide solutions of the complexes at room temperature or −20 °C. The structures of the present complexes have been elucidated by X-ray crystallography and the structural similarity of the whole series has been established.

Each crystal structure consists of a trinuclear cation $[(M_AL_2)_2M_B]^{2+}$, two perchlorate ions, two *N*,*N*-dimethylacetamide molecules, and two water or methanol molecules. A perspective drawing of the trinuclear cation of **1** is given in Fig. 1 as one of the examples. Selected bond distances and angles are listed in Tables 2, 3, 4, and 5. All the ten molecular structures contain a linear array of three metal atoms, with the central one on a crystallographic two-fold axis. The central M_B atom is linked to each M_A atom by two sulfur atom bridges, forming a distorted tetrahedral M_BS_4 geometry. On the other hand, the terminal M_A atoms have distorted octahedral $M_AN_4S_2$ geometries with a meridional bis-chelate of the thiolic ligands. The coordination geometry and the bridging mode of the thiolate ligand are constant over the whole series of structures, but show significant variation in the bond parameters. The terminal M_A–S and M_A–N distances of $[(M_AL_2)_2M_B]^{2+}$ [Mn–S 2.641(2)—2.675(3) Å, Mn–N 2.267(6)—2.289(9) Å; Fe–S 2.556(2)—2.578(2) Å, Fe–N 2.204(7)—2.230(8) Å; Co–S 2.527(2)—2.575(3) Å, Co–N 2.173(6)—2.207(7) Å] are comparable to the corresponding octahedral bond lengths of the homometal trinuclear cations, $[(M_AL_2)_2M_A]^{2+}$ [Mn–S 2.635(2)—2.661(2) Å, Mn–N 2.276(7)—2.306(6) Å;[35] Fe–S 2.546(3)—2.584(3) Å, Fe–N 2.18(1)—2.223(9) Å;[36] Co–S 2.509(4)—2.520(4) Å, Co–N 2.16(1)—2.20(1) Å[38]]. The central M_B–S dis-

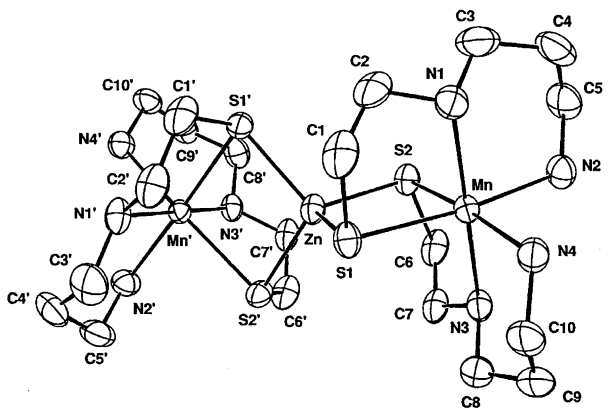

Fig. 1. A perspective view of the structure of $[(M_AL_2)_2M_B]^{2+}$ (M_A = Mn; M_B = Zn), showing the atom-labeling scheme.

Table 1. Crystal Data and Data Collection Details

Complex	$[(MnL_2)_2Zn](ClO_4)_2$ ·2dmac·$2CH_3OH$ (**1**)	$[(MnL_2)_2Cd](ClO_4)_2$ ·2dmac·$2H_2O$ (**2**)	$[(FeL_2)_2Zn](ClO_4)_2$ ·2dmac·$2CH_3OH$ (**3**)	$[(FeL_2)_2Cd](ClO_4)_2$ ·2dmac·$2H_2O$ (**4**)	$[(FeL_2)_2Hg](ClO_4)_2$ ·2dmac·$2H_2O$ (**5**)
Formula	$C_{30}H_{78}Cl_2Mn_2N_{10}O_{12}S_4Zn$	$C_{28}H_{74}CdCl_2Mn_2N_{10}O_{12}S_4$	$C_{30}H_{78}Cl_2Fe_2N_{10}O_{12}S_4Zn$	$C_{28}H_{74}CdCl_2Fe_2N_{10}O_{12}S_4$	$C_{28}H_{74}Cl_2Fe_2HgN_{10}O_{12}S_4$
F.W.	1145.5	1164.4	1145.5	1166.2	1254.4
Crystal system	Monoclinic	Monoclinic	Monoclinic	Monoclinic	Monoclinic
Space group	$C2/c$	$C2/c$	$C2/c$	$C2/c$	$C2/c$
a/Å	33.968(5)	33.661(5)	33.842(11)	33.573(6)	33.578(6)
b/Å	9.473(2)	9.479(1)	9.438(2)	9.448(1)	9.440(1)
c/Å	18.722(3)	19.015(3)	18.731(6)	18.898(3)	18.883(3)
β/°	117.83(1)	117.13(1)	118.13(1)	117.36(1)	117.17(1)
V/Å^3	5342(2)	5399(1)	5276(3)	5324(1)	5325(1)
Z	4	4	4	4	4
D_c/ g cm^{-3}	1.42	1.43	1.44	1.49	1.57
D_m/ g cm^{-3}	1.44	1.50	1.46	1.49	1.61
μ(Mo$K\alpha$)/ cm^{-1}	12.11	11.34	13.16	12.41	37.22
Crystal size/ mm	0.60 × 0.38 × 0.25	0.58 × 0.40 × 0.30	0.50 × 0.30 × 0.15	0.45 × 0.30 × 0.15	0.65 × 0.36 × 0.25
2θ range /°	2.0—48.0	2.0—48.0	2.0—49.0	2.0—49.0	2.0—48.0
Total no. of reflections measured	4475	4513	4664	4713	4438
No. of unique reflections with $I \geq 3\sigma(I)$	2448	2830	2460	2472	2934
R	0.049	0.059	0.058	0.050	0.046
R_w	0.054	0.073	0.064	0.058	0.055
Complex	$[(CoL_2)_2Zn](ClO_4)_2$ ·2dmac·$2CH_3OH$ (**6**)	$[(CoL_2)_2Cd](ClO_4)_2$ ·2dmac·$2H_2O$ (**7**)	$[(NiL_2)_2Zn](ClO_4)_2$ ·2dmac·$2CH_3OH$ (**8**)	$[(NiL_2)_2Cd](ClO_4)_2$ ·2dmac·$2H_2O$ (**9**)	$[(NiL_2)_2Hg](ClO_4)_2$ ·2dmac·$2H_2O$ (**10**)
Formula	$C_{30}H_{78}Cl_2Co_2N_{10}O_{12}S_4Zn$	$C_{28}H_{74}CdCo_2Cl_2N_{10}O_{12}S_4$	$C_{30}H_{78}Cl_2N_{10}Ni_2O_{12}S_4Zn$	$C_{28}H_{74}CdCl_2N_{10}Ni_2O_{12}S_4$	$C_{28}H_{74}Cl_2HgN_{10}Ni_2O_{12}S_4$
F.W.	1153.4	1172.4	1153.0	1171.9	1260.1
Crystal system	Monoclinic	Monoclinic	Monoclinic	Monoclinic	Monoclinic
Space group	$C2/c$	$C2/c$	$C2/c$	$C2/c$	$C2/c$
a/Å	33.759(6)	33.527(5)	33.726(5)	33.416(9)	33.389(6)
b/Å	9.403(1)	9.433(1)	9.349(2)	9.358(3)	9.370(1)
c/Å	18.748(3)	18.939(3)	18.802(3)	18.907(6)	18.881(4)
β/°	118.11(1)	117.22(1)	118.22(1)	117.18(1)	116.87(1)
V/Å^3	5249(1)	5327(1)	5224(1)	5259(3)	5269(2)
Z	4	4	4	4	4
D_c/ g cm^{-3}	1.46	1.46	1.47	1.48	1.59
D_m/ g cm^{-3}	1.46	1.48	1.47	1.51	1.62
μ(Mo$K\alpha$)/ cm^{-1}	14.01	13.17	14.98	14.24	39.29
Crystal size/ mm	0.61 × 0.28 × 0.21	0.45 × 0.29 × 0.21	0.30 × 0.29 × 0.22	0.43 × 0.29 × 0.20	0.40 × 0.32 × 0.31
2θ range /°	2.0—48.0	2.0—49.0	2.0—48.0	2.0—49.0	2.0—49.0
Total no. of reflections measured	4390	4709	4377	4661	4664
No. of unique reflections with $I \geq 3\sigma(I)$	2273	2884	2249	2624	2908
R	0.048	0.053	0.047	0.057	0.038
R_w	0.053	0.064	0.051	0.066	0.045

Table 2. Selected Interatomic Distances (l/Å) and Bond Angles (ϕ/°) of Mn-Series Complexes with Their Estimated Standard Deviations in Parentheses

	M_B = Mn[a]	M_B = Zn (**1**)	M_B = Cd (**2**)
Mn–M_B	3.420(1)	3.359(1)	3.500(1)
Mn–Mn′	6.839(2)	6.718(1)	6.998(1)
Mn–M_B–Mn′	180(0)	178.54(5)	177.40(4)
Mn–S1–M_B	84.71(6)	84.31(7)	84.61(9)
Mn–S2–M_B	84.00(6)	83.99(7)	84.28(9)
M_B–S1	2.435(2)	2.354(2)	2.532(3)
M_B–S2	2.442(2)	2.360(2)	2.539(3)
S1–M_B–S1′	120.24(8)	118.13(8)	116.8(1)
S1–M_B–S2	100.87(6)	103.16(6)	98.75(8)
S1–M_B–S2′	108.08(6)	107.52(7)	113.1(1)
S2–M_B–S2′	119.92(8)	118.12(8)	117.32(9)
Mn–S1	2.635(2)	2.641(2)	2.665(3)
Mn–S2	2.661(2)	2.651(2)	2.675(3)
Mn–N1	2.276(7)	2.274(7)	2.286(9)
Mn–N2	2.306(6)	2.267(6)	2.284(8)
Mn–N3	2.274(7)	2.270(6)	2.289(9)
Mn–N4	2.286(6)	2.268(6)	2.282(8)
S1–Mn–S2	90.42(6)	88.51(6)	92.26(8)
S1–Mn–N1	81.9(1)	82.1(2)	81.1(2)
S1–Mn–N2	171.2(2)	170.9(2)	170.0(3)
S1–Mn–N3	96.8(1)	96.2(1)	96.7(2)
S1–Mn–N4	93.1(2)	92.7(2)	91.15(2)
S2–Mn–N1	96.5(1)	95.8(2)	95.7(2)
S2–Mn–N2	89.3(1)	90.2(2)	89.8(2)
S2–Mn–N3	81.2(1)	82.4(2)	81.3(2)
S2–Mn–N4	169.8(2)	170.3(2)	168.5(2)
N1–Mn–N2	89.5(2)	89.1(2)	89.0(3)
N1–Mn–N3	177.4(2)	177.6(2)	176.2(2)
N1–Mn–N4	93.5(2)	94.0(2)	95.7(3)
N2–Mn–N3	91.8(2)	92.5(2)	93.2(3)
N2–Mn–N4	88.7(2)	90.1(2)	88.8(3)
N3–Mn–N4	88.9(2)	87.8(2)	87.4(3)

a) $[(MnL_2)_2Mn]Cl_2 \cdot 2CH_3OH$.[35b]

tances are also comparable to the corresponding tetrahedral M_B–S distances found in the similar homometal trinuclear cations or other tetrahedral thiolates [Zn–S in **1**, **3**, **6**, **8**: 2.344(2)—2.360(2) Å; Zn–S in $[Zn(ZnL'_2)_2](BF_4)_2$ (HL′ = 2-(2-pyridylmethylamino)ethanethiol): 2.347(3)—2.602(3) Å.[43] Cd–S in **2**, **4**, **7**, **9**: 2.513(3)—2.539(3) Å; Cd–S in $[Cd(CdL_2)_2]$: 2.534(4)—2.536(4) Å.[38] Hg–S in **5**, **10**: 2.519(2)—2.548(3) Å; Hg–S in $(Ph_4P)_2[Hg_3(SCH_2CH_2S)_4]$: 2.545(2)—2.563(2) Å[44)]. Structure **1**—**10** manifest a systematic change in the bond parameters as the terminal metal is varied from Mn to Ni, or the central metal is varied from Zn through Cd and Hg. The M_A–S distances decrease as M_A = Mn(II) > Fe(II) > Co(II) > Ni(II), which is the order of the Schannon high-spin octahedral radii [Mn(II) (0.97 Å) > Fe(II) (0.92 Å) > Co(II) (0.89 Å) > Ni(II) (0.83 Å)].[45] On the other hand, the M_B–S distances varies as M_B = Zn(II) < Cd(II) > Hg(II), which is not the order of the Schannon tetrahedral radii [Zn(II) (0.74 Å) < Cd(II) (0.92 Å) < Hg(II) (1.10 Å)].[45] The unexpectedly short Hg(II)–S bonds in **5** and **10** may be due to a great affinity of the thiolate sulfur to the mercury atom. The bridging angles M_A–S–M_B are 83.9(1)—88.1(1)° in the Mn, Fe, Co, and Ni series ($[(MnL_2)_2M_B]^{2+}$, $[(FeL_2)_2M_B]^{2+}$, $[(CoL_2)_2M_B]^{2+}$, and $[(NiL_2)_2M_B]^{2+}$) and increases as M_B = Zn(II) < Cd(II) < Hg(II) in each series.

The perchlorate ion is in the vicinity of the amino nitrogen atom of the thiolic ligand and methanol or water molecules, as indicated by the distances $[O(ClO_4)\cdots N(L)$ 3.16(1)—3.45(1) Å, $O(ClO_4)\cdots O(CH_3OH)$ 3.09(2)—3.23(3) Å, and $O(ClO_4)\cdots O(H_2O)$ 3.42(3)—3.47(3) Å], which suggest the occurrence of hydrogen bondings. The amino nitrogen atoms of the thiolic ligand are further hydrogen bonded to the dimethylacetamide molecules, as implied by the N(L)···O(dmac) distances of 2.938(9)—3.02(1) Å.

The synthesis of the heterometal complexes has the advantage of permitting a clear interpretation of the electronic spectral features to the first approximation. The diffuse reflectance spectra of the Mn-series complexes (**1** and **2**) are shown in Fig. 2, together with those of the corresponding homometal trinuclear complexes $[(MnL_2)_2Mn]^{2+}$[35)] and $[(CdL_2)_2Cd]^{2+}$.[38] The spectrum of $[(MnL_2)_2Mn]^{2+}$ shows four peaks (437, 473, 499, and 628 nm), which are not observed for **1**, **2**, and $[(CdL_2)_2Cd]^{2+}$, in the visible and near-infrared region. These absorptions could not be observed in the solution spectra and therefore they should be attributed to the spin-forbidden d–d transitions of the high-spin manganese(II) ion in a tetrahedral environment based on the comparison of these spectra. The two absorptions (1194 and 1556 nm) in the near-infrared region may be due to vibronic bands in the thiolate-bridged trinuclear framework. The diffuse reflectance spectra of the Fe series (**3**, **4**, and **5**) and the trinuclear Fe(II) complex, $[(FeL_2)Fe]^{2+}$,[36)] are shown in Fig. 3. In the Fe series, the spectra are characterized by two broad absorptions around 870—918 and 1029—1066 nm in the near-infrared region, which can be associated with d–d transitions based on the $^5T_{2g} \rightarrow {}^5E_g$ transitions.[46)] The extra band around 1650 nm in $[(FeL_2)Fe]^{2+}$ should be due to the tetrahedral Fe(II) and

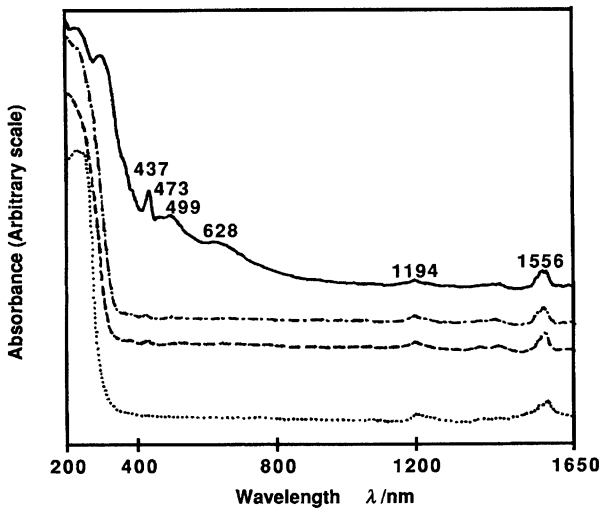

Fig. 2. Diffuse reflectance spectra of Mn-series complexes and cadmium complex. $[(MnL_2)_2Mn]^{2+}$ [35b)] (—), $[(MnL_2)_2Zn]^{2+}$ (**1**) (- - -), $[(MnL_2)_2Cd]^{2+}$ (**2**) (–·–), $[(CdL_2)_2Cd]^{2+}$ [38)] (···).

Table 3. Selected Interatomic Distances (l/Å) and Bond Angles (ϕ/°) of Fe-Series Complexes with Their Estimated Standard Deviations in Parentheses

	M_B = Fe[a]	M_B = Zn (**3**)	M_B = Cd (**4**)	M_B = Hg (**5**)
Fe–M_B	3.311(1)	3.297(1)	3.433(1)	3.464(1)
Fe–Fe′	6.623(1)	6.593(1)	6.864(1)	6.924(1)
Fe–M_B–Fe′	180.(0)	178.21(5)	177.05(4)	176.54(3)
Fe–S1–M_B	85.0(1)	84.4(1)	84.8(1)	85.5(1)
Fe–S2–M_B	83.9(1)	83.9(1)	84.3(1)	85.0(1)
M_B–S1	2.349(3)	2.348(2)	2.518(2)	2.531(3)
M_B–S2	2.362(3)	2.351(2)	2.529(3)	2.548(3)
S1–M_B–S1′	120.8(1)	119.2(1)	119.07(8)	119.65(9)
S1–M_B–S2	100.88(9)	101.35(7)	96.76(7)	95.58(8)
S1–M_B–S2′	107.9(1)	108.33(9)	113.25(9)	114.23(9)
S2–M_B–S2′	119.8(1)	119.3(1)	119.29(9)	119.34(8)
Fe–S1	2.546(3)	2.556(2)	2.575(3)	2.574(3)
Fe–S2	2.584(3)	2.573(2)	2.584(3)	2.578(3)
Fe–N1	2.18(1)	2.224(8)	2.215(8)	2.222(8)
Fe–N2	2.223(9)	2.224(7)	2.216(7)	2.215(8)
Fe–N3	2.222(9)	2.222(7)	2.230(8)	2.219(8)
Fe–N4	2.212(8)	2.204(7)	2.213(7)	2.217(7)
S1–Fe–S2	90.15(9)	90.28(7)	94.01(8)	93.81(8)
S1–Fe–N1	84.0(3)	83.3(1)	82.3(2)	82.3(2)
S1–Fe–N2	174.6(3)	173.2(2)	172.4(2)	172.5(2)
S1–Fe–N3	96.9(2)	96.4(2)	97.0(2)	96.6(2)
S1–Fe–N4	91.9(3)	91.4(2)	89.5(2)	89.5(2)
S2–Fe–N1	95.9(2)	95.9(2)	95.2(2)	95.0(2)
S2–Fe–N2	88.7(2)	89.4(2)	88.2(1)	88.2(2)
S2–Fe–N3	82.5(2)	83.8(2)	83.2(2)	83.2(2)
S2–Fe–N4	172.5(3)	171.9(2)	171.3(2)	171.2(2)
N1–Fe–N2	90.9(4)	90.0(3)	90.3(3)	90.3(3)
N1–Fe–N3	178.2(4)	179.6(1)	178.2(2)	177.9(2)
N1–Fe–N4	91.5(4)	92.1(3)	93.1(3)	93.4(3)
N2–Fe–N3	88.2(4)	90.3(3)	90.4(3)	90.8(3)
N2–Fe–N4	89.9(3)	89.9(2)	89.3(3)	89.5(3)
N3–Fe–N4	90.1(3)	88.2(3)	88.5(3)	88.4(3)

a) $[(FeL_2)_2Fe]Cl_2 \cdot 2CH_3OH$.[36]

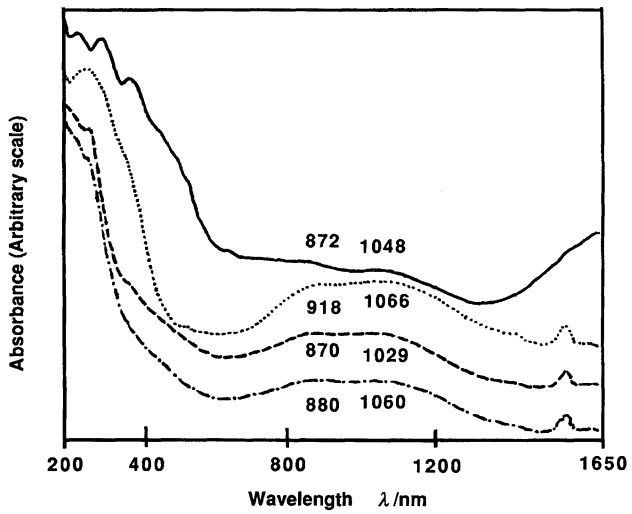

Fig. 3. Diffuse reflectance spectra of Fe-series complexes. $[(FeL_2)_2Fe]^{2+}$ [36] (—), $[(FeL_2)_2Zn]^{2+}$ (**3**) (- - -), $[(FeL_2)_2Cd]^{2+}$ (**4**) (–·–), $[(FeL_2)_2Hg]^{2+}$ (**5**) (···).

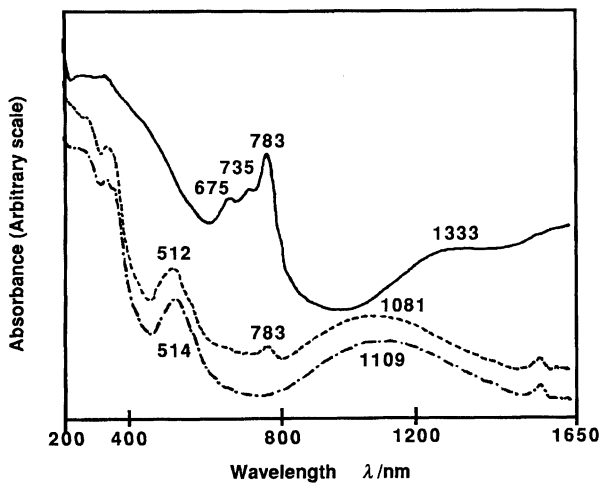

Fig. 4. Diffuse reflectance spectra of Co-series complexes. $[(CoL_2)_2Co]^{2+}$ [37] (—), $[(CoL_2)_2Zn]^{2+}$ (**6**) (- - -), $[(CoL_2)_2Cd]^{2+}$ (**7**) (–·–).

assigned as $^5E \rightarrow {}^5T_2$ transition.[46] In Fig. 4, the diffuse reflectance spectra of the Co series (**6** and **7**) are shown together with that of the trinuclear Co(II) complex, $[(CoL_2)Co]^{2+}$.[38] The two absorptions (512 and 1081 nm for **6**, 514 and 1109

Table 4. Selected Interatomic Distances (l/Å) and Bond Angles (ϕ/°) of Co-Series Complexes with Their Estimated Standard Deviations in Parentheses

	M_B = Co[a)]	M_B = Zn (**6**)	M_B = Cd (**7**)
Co–M_B	3.236(1)	3.295(1)	3.462(1)
Co–Co′	6.472(2)	6.588(1)	6.921(1)
Co–M_B–Co′	178.0(1)	178.01(5)	176.80(4)
Co–S1–M_B	84.4(1)	85.0(1)	85.5(1)
Co–S2–M_B	83.9(1)	84.8(1)	85.3(1)
M_B–S1	2.304(4)	2.346(2)	2.523(2)
M_B–S2	2.313(4)	2.351(2)	2.536(2)
S1–M_B–S1′	119.9(2)	120.34(9)	119.71(9)
S1–M_B–S2	101.2(2)	99.76(7)	95.59(7)
S1–M_B–S2′	108.2(1)	108.91(8)	113.85(9)
S2–M_B–S2′	119.2(1)	120.51(9)	120.05(9)
Co–S1	2.509(4)	2.527(2)	2.575(3)
Co–S2	2.520(4)	2.533(2)	2.574(3)
Co–N1	2.160(13)	2.187(7)	2.200(8)
Co–N2	2.198(10)	2.173(6)	2.197(7)
Co–N3	2.158(12)	2.186(7)	2.207(8)
Co–N4	2.199(11)	2.186(6)	2.207(7)
S1–Co–S2	90.4(1)	90.44(7)	93.42(8)
S1–Co–N1	84.0(3)	84.1(2)	82.4(2)
S1–Co–N2	174.4(4)	174.4(2)	172.7(2)
S1–Co–N3	96.9(3)	95.9(2)	96.4(2)
S1–Co–N4	91.4(3)	91.0(2)	89.4(2)
S2–Co–N1	95.6(3)	95.1(2)	94.8(2)
S2–Co–N2	89.8(3)	89.6(2)	89.0(2)
S2–Co–N3	84.2(3)	84.4(2)	83.0(2)
S2–Co–N4	173.0(4)	173.5(2)	171.6(2)
N1–Co–N2	90.5(5)	90.3(3)	90.5(3)
N1–Co–N3	179.1(5)	179.5(2)	177.5(2)
N1–Co–N4	91.3(4)	91.4(2)	93.4(3)
N2–Co–N3	88.6(4)	89.7(2)	90.7(3)
N2–Co–N4	89.1(4)	89.6(2)	89.2(3)
N3–Co–N4	88.9(5)	89.1(2)	88.8(3)

a) $[(CoL_2)_2Co](ClO_4)_2 \cdot 2dmac \cdot 2CH_3OH$.[38)]

Table 5. Selected Interatomic Distances (l/Å) and Bond Angles (ϕ/°) of Ni-Series Complexes with Their Estimated Standard Deviations in Parentheses

	M_B = Zn (**8**)	M_B = Cd (**9**)	M_B = Hg (**10**)
Ni–M_B	3.305(1)	3.461(1)	3.498(1)
Ni–Ni′	6.610(1)	6.918(1)	6.991(1)
Ni–M_B–Ni′	177.78(5)	176.22(4)	175.6(3)
Ni–S1–M_B	85.7(1)	86.9(1)	88.1(1)
Ni–S2–M_B	85.9(1)	86.6(1)	87.6(1)
M_B–S1	2.344(2)	2.513(3)	2.519(2)
M_B–S2	2.352(2)	2.530(3)	2.546(2)
S1–M_B–S1′	121.69(9)	122.52(9)	124.03(7)
S1–M_B–S2	98.16(7)	93.06(8)	91.52(6)
S1–M_B–S2′	109.45(8)	114.23(9)	115.11(8)
S2–M_B–S2′	121.66(9)	122.3(1)	122.57(7)
Ni–S1	2.503(2)	2.519(3)	2.511(2)
Ni–S2	2.506(2)	2.517(3)	2.508(2)
Ni–N1	2.136(7)	2.136(9)	2.140(7)
Ni–N2	2.139(6)	2.134(8)	2.136(6)
Ni–N3	2.135(7)	2.137(8)	2.134(7)
Ni–N4	2.146(6)	2.143(7)	2.142(6)
S1–Ni–S2	90.21(7)	93.24(8)	92.62(7)
S1–Ni–N1	84.7(2)	84.0(2)	83.8(2)
S1–Ni–N2	176.0(2)	175.2(2)	175.4(2)
S1–Ni–N3	94.8(2)	95.1(2)	94.9(2)
S1–Ni–N4	90.5(2)	89.3(2)	89.4(2)
S2–Ni–N1	94.0(2)	93.5(2)	93.7(2)
S2–Ni–N2	89.4(2)	88.7(2)	88.9(2)
S2–Ni–N3	84.8(2)	84.4(2)	84.8(2)
S2–Ni–N4	175.0(2)	174.2(2)	174.6(2)
N1–Ni–N2	91.3(3)	91.5(3)	91.7(3)
N1–Ni–N3	178.7(2)	177.6(2)	178.0(2)
N1–Ni–N4	91.0(3)	92.0(3)	91.5(3)
N2–Ni–N3	89.2(3)	89.4(3)	89.6(2)
N2–Ni–N4	90.2(2)	89.2(2)	89.5(2)
N3–Ni–N4	90.2(3)	90.2(3)	90.1(3)

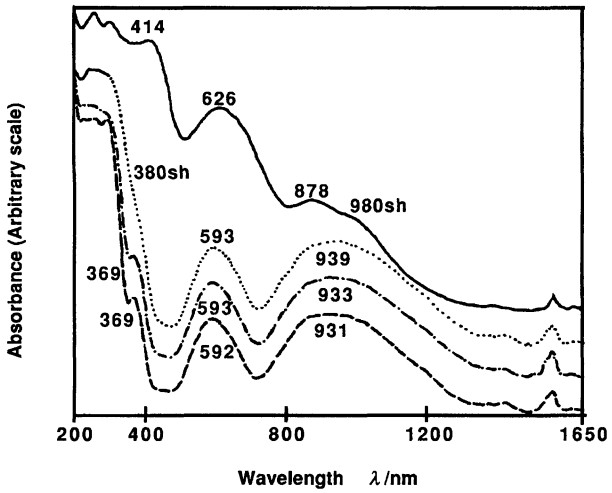

Fig. 5. Diffuse reflectance spectra of Ni-series complexes. $[(NiL_2)_2Ni]^{2+}$ [37)] (——), $[(NiL_2)_2Zn]^{2+}$ (**8**) (- - -), $[(NiL_2)_2Cd]^{2+}$ (**9**) (– · –), $[(NiL_2)_2Hg]^{2+}$ (**10**) (· · ·).

nm for **7**) which are not obscure in $[(CoL_2)Co]^{2+}$ should be due to the octahedral Co(II) and assigned to $^4T_{1g} \rightarrow {}^4T_{1g}(P)$ and $^4T_{1g} \rightarrow {}^4T_{2g}$, respectively.[46)] From the comparison of the spectra we can consider that the d–d absorptions of the central tetrahedral Co(II) of $[(CoL_2)Co]^{2+}$ appear at 675, 735, 783, and 1333 nm. The former three absorptions should be assigned to $^4A_2 \rightarrow {}^4T_1(P)$ and the latter one to $^4A_2 \rightarrow {}^4T_1(F)$.[46)] In **6**, a weak absorption appears at 783 nm; this may be due to the tetrahedral Co(II). This results shows a small amount of homometal species $[(CoL_2)Co]^{2+}$ which we could not exclude was contaminated in the sample of **6**. Based on the intensities of this absorption in the solution spectra, we estimate the amount of the homometal species to be about 0.5%. In the Ni series, the spectra (Fig. 5) are characterized by the three absorption bands (369, 592, 931 nm for **8**; 369, 593, 933 nm for **9**; 380sh, 593, 939 nm for **10**), which can be assigned as $^3A_{2g} \rightarrow {}^3T_{1g}(P)$, $^3A_{2g} \rightarrow {}^3T_{1g}(F)$, $^3A_{2g} \rightarrow {}^3T_{2g}$ transitions, respectively.[46)]

In the present series of complexes, the central atom, M_B, has d^{10} electronic configuration. Thus, one might expect that magnetic interaction between the two terminal atoms, M_A and M'_A operates via the central metal atom M_B. The magnetic susceptibilities of the present complexes were measured over the temperature rage 80—300 K; the results are

shown in Figs. 6, 7, 8, and 9. In the Mn series, the magnetic moments of **1** and **2** are 8.54 and 8.66 B.M., respectively, at room temperature, which are comparable to the spin-only value (8.37 B.M.) for a d^5 (high-spin)–d^{10}–d^5 (high-spin) system. The temperature dependence of magnetic data show a Curie-law behavior, $\chi_A = C/(T-\theta)$, with very small Weiss constants (θ=0.27 and −0.32 K for **1** and **2**, respectively) as shown in Fig. 6. This indicates that the magnetic interaction between the two terminal manganese atoms is very weak. In the Fe series, the effective magnetic moments of **3**, **4**, and **5** are 8.15, 7.73, and 7.84 B.M., respectively, at room temperature. These values are higher than the spin-only value 6.93 B.M. for a d^6 (high-spin)–d^{10}–d^6 (high-spin) system. This should be due to orbital contribution to the magnetic moments of complexes with the $^5T_{2g}$ ground term. For example, if we use a magnetic moment of 5.6 B.M. for the iron(II) ions to take account of the orbital contribution,[47,48] the

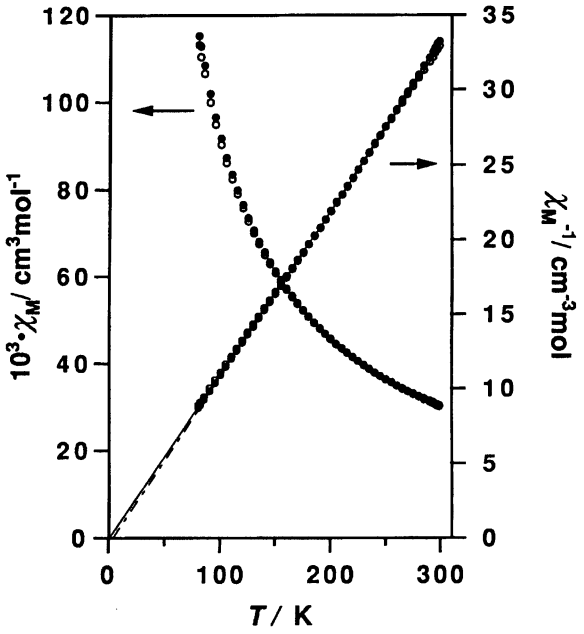

Fig. 6. Magnetic susceptibility data of Mn-series complexes. $[(MnL_2)_2Zn]^{2+}$ (**1**) (○), $[(MnL_2)_2Cd]^{2+}$ (**2**) (●).

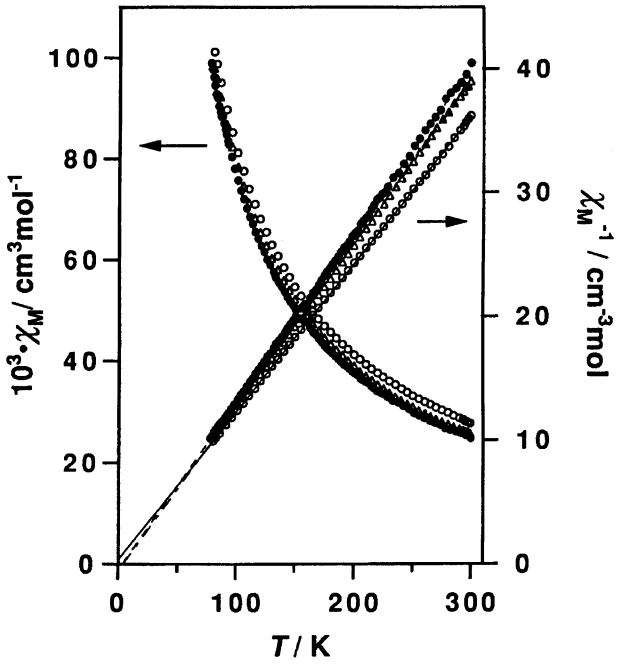

Fig. 7. Magnetic susceptibility data of Fe-series complexes. $[(FeL_2)_2Zn]^{2+}$ (**3**) (○), $[(FeL_2)_2Cd]^{2+}$ (**4**) (●), $[(FeL_2)_2Hg]^{2+}$ (**5**) (△).

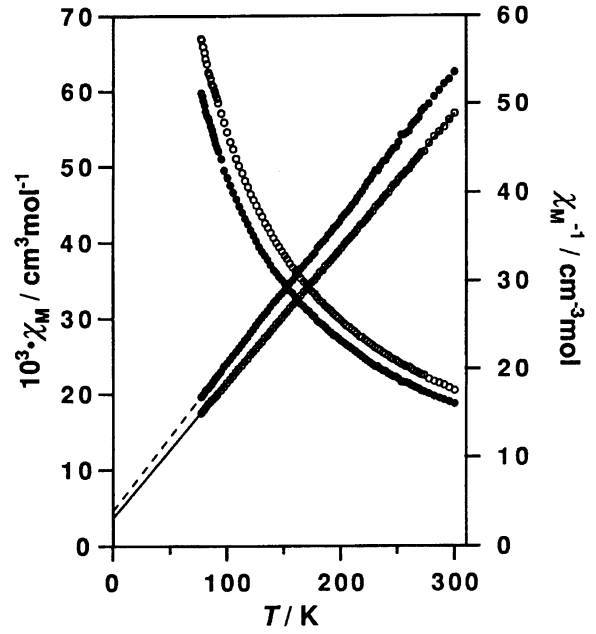

Fig. 8. Magnetic susceptibility data of Co-series complexes. $[(CoL_2)_2Zn]^{2+}$ (**6**) (○), $[(CoL_2)_2Cd]^{2+}$ (**7**) (●).

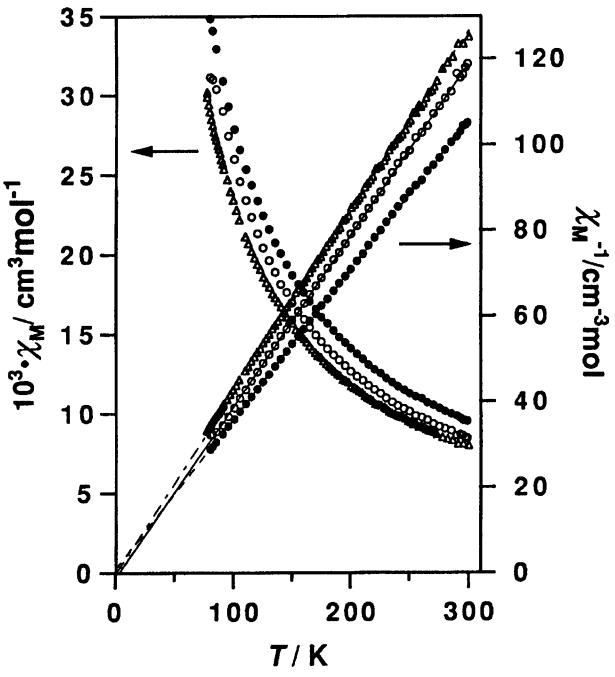

Fig. 9. Magnetic susceptibility data of Ni-series complexes. $[(NiL_2)_2Zn]^{2+}$ (**8**) (○), $[(NiL_2)_2Cd]^{2+}$ (**9**) (●), $[(NiL_2)_2Hg]^{2+}$ (**10**) (△).

expected value for the Fe-series complexes become 7.9 B.M. and comparable to the observed moments. As can be seen in Fig. 7, the magnetic data obey the Curie–Weiss law, $\chi_M = C/(T-\theta)$, with a small Weiss constants ($\theta = -2.6$, 3.2, and 4.5 K for **3**, **4**, and **5**, respectively). This shows that the magnetic interaction between the two terminal metal atoms is weak. In the Co series, the magnetic moments of **6** and **7** are 7.01 and 6.65 B.M., respectively, at room temperature, which are considerably higher than the spin-only value 5.48 B.M. for a d^7 (high-spin)–d^{10}–d^7 (high-spin) system. These large values can be attributed to an orbital contribution of the $^4T_{1g}$ ground term. When we take a typical magnetic moment (5.2 B.M.) for an octahedral high-spin cobalt(II),[47,48] the magnetic moments of the Co-series complexes can be calculated to be 7.4 B.M., which is close to the observed values. The magnetic data obey the Curie–Weiss law with negative Weiss constants ($\theta = -21$ and -24 K for **6** and **7**, respectively). One of the possible explanations for the magnetic behavior may be that an antiferromagnetic interaction between the two terminal cobalt atoms is operating through the central M_B metal atom. However, in this system this is not the case. The θ values are comparable to those of some octahedrally coordinated high-spin cobalt(II) compounds and the magnetic moments of typical octahedral cobalt(II) ions should depend appreciably on temperature.[47,48] In the Ni series, the room-temperature magnetic moments of **8**, **9**, and **10** are 4.51, 4.77, and 4.36 B.M., respectively, showing values a little larger than the spin-only magnetic moments (4.00 B.M.) for a d^8 (high-spin)–d^{10}–d^8 (high-spin) system. The larger values can be due to the spin-orbit coupling of $^3A_{2g}$ ground term.[46,47] The magnetic data obey the Curie–Weiss law, $\chi_M = C/(T-\theta)$, with small Weiss constants ($\theta = 3.1$, -2.2, and 0.65 K for **8**, **9**, and **10**, respectively), showing that the magnetic interaction between the Ni atoms is weak (Fig. 9). As a whole the magnetic interaction between the two terminal metal atoms is negligibly small or weak in the preset series of thiolato-bridged complexes possibly because of the rather long distances of the two terminal atoms (6.472(2)—6.998(1) Å).

This work partially supported by a Grant-in-Aid for Scientific Research No. 08404046 from the Ministry of Education, Science, Sports and Culture.

References

1) D. C. Jicha and D. H. Busch, *Inorg. Chem.*, **1**, 872 (1962).
2) D. C. Jicha and D. H. Busch, *Inorg. Chem.*, **1**, 878 (1962).
3) D. H. Busch and D. C. Jicha, *Inorg. Chem.*, **1**, 884 (1962).
4) C. H. Wei and L. F. Dahl, *Inorg. Chem.*, **9**, 1878 (1970).
5) G. R. Brubaker and B. E. Douglas, *Inorg. Chem.*, **6**, 1562 (1967).
6) G. Freeh, K. Chapman, and E. L. Blinn, *Inorg. Nucl. Chem. Lett.*, **9**, 91 (1973).
7) E. L. Blinn, P. Butler, K. M. Chapman, and S. Harris, *Inorg. Chim. Acta*, **24**, 139 (1977).
8) P. Butler and E. L. Blinn, *Inorg. Chem.*, **17**, 2037 (1978).
9) G. R. Brubaker and D. W. Johnson, *Inorg. Chim. Acta*, **100**, 201 (1985).
10) M. J. Heeg, E. L. Blinn, and E. Deutsch, *Inorg. Chem.*, **24**, 1118 (1985).
11) D. W. Johnson and T. R. Brewer, *Inorg. Chim. Acta*, **154**, 221 (1988).
12) T. Konno, S. Aizawa, and J. Hidaka, *Bull. Chem. Soc. Jpn.*, **62**, 585 (1989).
13) T. Konno, S. Aizawa, K. Okamoto, and J. Hidaka, *Bull. Chem. Soc. Jpn.*, **63**, 792 (1990).
14) a) T. Konno, K. Okamoto, and J. Hidaka, *Chem. Lett.*, **1990**, 1043; b) T. Konno, K. Okamoto, and J. Hidaka, *Bull. Chem. Soc. Jpn.*, **67**, 101 (1994).
15) T. Konno, K. Okamoto, and J. Hidaka, *Bull. Chem. Soc. Jpn.*, **63**, 3027 (1990).
16) a) T. Konno, K. Okamoto, and J. Hidaka, *Inorg. Chem.*, **30**, 2253 (1991); b) T. Konno, T. Nagashio, K. Okamoto, and J. Hidaka, *Inorg. Chem.*, **31**, 1160 (1992); c) T. Konno, K. Okamoto, and J. Hidaka, *Inorg. Chem.*, **33**, 538 (1994).
17) a) T. Konno, K. Okamoto, and J. Hidaka, *Inorg. Chem.*, **31**, 160 (1992); b) T. Konno, J. Hidaka, and K. Okamoto, *Bull. Chem. Soc. Jpn.*, **68**, 1353 (1995).
18) a) K. Okamoto, T. Konno, Y. Kageyama, and J. Hidaka, *Chem. Lett.*, **1992**, 1105; b) K. Okamoto, Y. Kageyama, and T. Konno, *Bull. Chem. Soc. Jpn.*, **68**, 2573 (1995).
19) T. Konno, K. Okamoto, and J. Hidaka, *Inorg. Chem.*, **31**, 3875 (1992).
20) T. Konno, K. Okamoto, and J. Hidaka, *Acta Crystallogr., Sect. C*, **49**, 222 (1993).
21) T. Konno, K. Nakamura, K. Okamoto, and J. Hidaka, *Bull. Chem. Soc. Jpn.*, **66**, 2582 (1993).
22) T. Konno, K. Yonenobu, J. Hidaka, and K. Okamoto, *Inorg. Chem.*, **33**, 861 (1994).
23) K. Okamoto, T. Konno, and J. Hidaka, *J. Chem. Soc., Dalton Trans.*, **1994**, 533.
24) T. Konno, Y. Kageyama, and K. Okamoto, *Bull. Chem. Soc. Jpn.*, **67**, 1957 (1994).
25) T. Konno and K. Okamoto, *Bull. Chem. Soc. Jpn.*, **68**, 610 (1995).
26) T. Yonemura, K. Okamoto, T. Ama, H. Kawaguchi, and T. Yasui, *Chem. Lett.*, **1993**, 1123.
27) S. L. Rose, R. E. Hoskin, J. E. Cavanaugh, C. J. Smith, and E. L. Blinn, *Inorg. Chim. Acta*, **40**, 7 (1980).
28) M. Handa, H. Okawa, and S. Kida, *Bull. Chem. Soc. Jpn.*, **61**, 3353 (1988).
29) M. Mikuriya, S. Kida, and I. Murase, *Bull. Chem. Soc. Jpn.*, **60**, 1180 (1987).
30) M. Handa, M. Mikuriya, Z. J. Zhong, H. Okawa, and S. Kida, *Bull. Chem. Soc. Jpn.*, **61**, 3883 (1988).
31) M. Mikuriya, S. Shigematsu, M. Handa, and T. Kohzuma, *Transition Met. Chem.*, **16**, 532 (1991).
32) a) M. Handa, M. Mikuriya, H. Okawa, and S. Kida, *Chem. Lett.*, **1988**, 1555; b) M. Mikuriya, M. Handa, S. Shigematsu, S. Funaki, T. Fujii, H. Okawa, K. Toriumi, T. Koshiba, and H. Terauchi, *Bull. Chem. Soc. Jpn.*, **66**, 1104 (1993).
33) M. Handa, M. Mikuriya, and H. Okawa, *Chem. Lett.*, **1989**, 1663.
34) M. Mikuriya, M. Handa, S. Shigematsu, S. Funaki, F. Adachi, and H. Okawa, *Bull. Chem. Soc. Jpn.*, **65**, 512 (1992).
35) a) M. Mikuriya, F. Adachi, H. Iwasawa, M. Handa, M. Koikawa, and H. Okawa, *Inorg. Chim. Acta*, **179**, 3 (1991); b) M. Mikuriya, F. Adachi, H. Iwasawa, M. Handa, M. Koikawa, and H. Okawa, *Bull. Chem. Soc. Jpn.*, **67**, 3263 (1994).
36) M. Mikuriya, T. Kotera, F. Adachi, M. Handa, M. Koikawa,

and H. Okawa, *Bull. Chem. Soc. Jpn.*, **68**, 574 (1995).
37) T. Kawahashi, H. Tsutsumi, and M. Mikuriya, *Polyhedron*, **15**, 169 (1996).
38) M. Mikuriya et al., Manuscript in preparation.
39) C. L. Spiro, S. L. Lambert, T. J. Smith, E. N. Duesler, R. R. Gagne, and D. N. Hendrickson, *Inorg. Chem.*, **20**, 1229 (1981).
40) W. J. Geary, *Coord. Chem. Rev.*, **7**, 81 (1971).
41) P. W. Selwood, "Magnetochemistry," Interscience Publishers, New York (1956), pp. 78 and 91.
42) C. K. Fair, "MolEN Structure Determination System," Delft Instruments, Delft, The Netherlands (1990).
43) U. Brand and H. Vahrenkamp, *Inorg. Chem.*, **34**, 3285 (1995).
44) G. Henkel, P. Betz, and B. Krebs, *J. Chem. Soc., Chem. Commun.*, **1985**, 1498.
45) a) R. D. Shannon and C. T. Prewitt, *Acta Crystallogr., Sect. B*, **25**, 925 (1969); b) R. D. Shannon, *Acta Crystallogr., Sect. A*, **32**, 751 (1976).
46) Y. Murakami and K. Sakata, "Kireto Kagaku," ed by K. Ueno, Nankodo, Tokyo (1976), Vol. 1, Chap. 2.
47) F. E. Mabbs and D. J. Machin, "Magnetism and Transition Metal Complexes," Chapman and Hall, London (1973), Chap. 4.
48) E. A. Boudreaux and L. N. Mulay, "Theory and Applications of Molecular Paramagnetism," John Wiley & Sons, Inc., New York (1976), Chap. 3.